Environmental Science & Technology Letters

pubs.acs.org/journal/estlcu

Letter

Chemically Induced Decline in Wintertime SO_2 Emission Control Efficacy

Fanghe Zhao, Yuhang Wang,* and Shengjun Xi

Cite This: *Environ. Sci. Technol. Lett.* 2025, 12, 1190−1196

Read Online

ACCESS | Metrics & More | Article Recommendations | Supporting Information

ABSTRACT: The reduction of SO_2 emissions from 2004 to 2023 has resulted in significant decreases in SO_2 and sulfate concentrations across the Rust Belt and Southeast of the United States, regions with coal-combustion power plant emissions. While the observed sulfate-to-total-sulfur ratio remained relatively constant at ∼30% in summer, this fraction increased from ∼10% to ∼20% in winter from 2004 to 2013 and then remained at ∼20%. The rise in sulfate-to-total-sulfur ratio resulted in a slower decrease of sulfate in 2004−2013 compared to 2013−2023 despite a greater reduction of SO_2 in the earlier decade, reflecting a significant decline in the efficacy of SO_2 emission reduction in improving air quality in winter. The decrease in efficacy is attributed to the increased oxidation of SO_2 in winter because of the diminishing oversupply of SO_2 compared to the availability of atmospheric oxidant, H_2O_2. Consequently, the seasonal differences in SO_2 and sulfate concentrations between summer and winter have narrowed. This chemical damping effect, caused by limited oxidant availability, is likely to delay the reduction in sulfate concentrations in other polluted regions where the transition from coal to natural gas in power plants or alternative energy sources has not progressed as rapidly as in the United States.

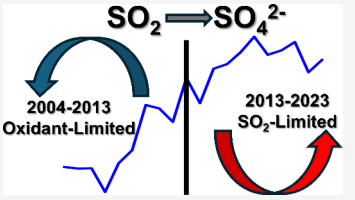

KEYWORDS: *SO_2 Emission Control, Sulfate Formation, Oxidant-Limited Regime, Power Plant Transitions, Machine Learning Analysis*

1. INTRODUCTION

Sulfate aerosols, primarily originating from sulfur dioxide (SO_2) emissions, are a significant contributor to air pollution and pose substantial health risks.[1−4] SO_2 emissions mainly come from power plants, particularly those burning coal and oil.[5−7] Sulfate aerosols from the oxidation of SO_2 contribute significantly to particulate matter with a size <2.5 μm (PM2.5), impacting air quality, health, visibility, and climate.[8,9] The widespread impacts of sulfate pollution have led to stringent emission control policies across industrialized nations, resulting in substantial reductions in SO_2 emissions from power plants in recent decades.[10,11] This emission reduction has resulted in improved health outcomes. A previous study estimated that mortality risk from exposure to coal PM2.5 decreased from 25% of all PM2.5 before 2009 to 7% after 2012 in the United States.[12,13]

The oxidation of SO_2 to sulfate occurs through multiple pathways in the atmosphere, including gas-phase oxidation by hydroxyl radicals (OH) and aqueous-phase oxidation by hydrogen peroxide (H_2O_2) or ozone (O_3) in cloud droplets or on aerosol surfaces.[3,14−17] A recent work by Gao et al.[18] demonstrated that H_2O_2-mediated oxidation dominates SO_2-to-sulfate conversion in the eastern United States, in contrast to regions like West Asia where transition metal ion (TMI)-catalyzed oxidation plays a more significant role.

Long-term monitoring efforts have revealed substantial declines in both SO_2 emissions and sulfate concentrations across North America and Europe.[10] In the United States, SO_2 emissions have decreased by over 90% since the enactment of the Clean Air Act Amendments in 1990.[19] Notably, the most significant decreases in both SO_2 and sulfate occurred in the Southeast from 1990 to 2015.[20] Previous studies have mostly focused on summertime reductions in SO_2 and sulfate concentrations.[10,11,20] However, the seasonal differences have not been studied extensively. An early study indicated considerably less reduction in observed sulfate concentrations in winter than summer in the 1990s.[21]

In this analysis, we analyze two decades (2004−2023) of SO_2 and sulfate observations over the Rust Belt and Southeast regions, which collectively house 72% of U.S. coal power plants. Our objective is to examine the distinct responses of SO_2 and sulfate concentrations to the reduction in SO_2 emissions in summer and winter.

2. MATERIALS AND METHODS

2.1. Data Sources and Processing. Long-term sulfate concentration data were obtained from the Interagency Monitoring of Protected Visual Environments (IMPROVE) network for Class I areas of national parks and wilderness areas across the United States[22,23] (Supporting Information Figure S1). The IMPROVE network provides 24-h integrated PM2.5

Received: July 22, 2025
Revised: August 6, 2025
Accepted: August 8, 2025
Published: August 18, 2025

samples collected every third day. We applied the IMPROVE data quality flags to exclude data affected by quality control failures or potential contamination.[24,25] Concurrent daily average SO_2 concentration data were computed using the observations from the EPA's Air Quality System (AQS), which underwent similar quality control procedures. The AQS measurements within a radius of 100 km were used to compute the averages (Supporting Information Figure S2). This proximity-based matching approach accounts for the spatial mismatch between IMPROVE sites (located in remote Class I areas) and AQS sites (primarily in populated areas). It also captures regional-scale transport and mixing processes that govern SO_2-to-sulfate transformation over atmospheric lifetimes of several days. To calculate power plant SO_2 emissions, we used the SO_2 emissions data from individual power plants, which were obtained from the EPA Hourly Continuous Emission Monitoring System (CEMS) (Supporting Information Figure S3).

To characterize the atmospheric oxidation environment, we used ECMWF Atmospheric Composition Reanalysis 4 (EAC4), which provided several key oxidant-related variables including H_2O_2 column abundance, H_2O_2 concentrations, and HO_2 concentrations at a 0.75° × 0.75° horizontal resolution with a 3-hly temporal resolution.[26] Additionally, we obtained supporting meteorological data from ERA5 (ECMWF Reanalysis v5) at matching spatial and temporal resolutions of EAC4.[27]

We calculated the supply of H_2O_2 for SO_2 oxidation through chemical production and advection. The primary chemical production rate, P, is that of HO_2 self-reactions, which depend on temperature, water vapor mixing ratios, and pressure:[28]

$$HO_2 + HO_2 \rightarrow H_2O_2 + O_2 \quad \text{(R1)}$$

The net advection rate, C, is the average of H_2O_2 convergence rate within planetary boundary layer

$$C = -\nabla\cdot(\vec{u}[H_2O_2]) \quad (1)$$

where $\vec{u}$ is the horizontal wind vector and $[H_2O_2]$ is the H_2O_2 concentration. The change of H_2O_2 concentrations can be written as

$$\frac{\partial[H_2O_2]}{\partial t} = P + C - L_{SO_2} - L_c - L_{dep} \quad (2)$$

where L_{SO_2} is the loss of H_2O_2 by oxidation of SO_2, L_c is the loss of H_2O_2 by other chemical reactions such as photolysis and reaction with OH, and L_{dep} is the loss by dry and wet deposition. To diagnose the SO_2 oxidation regime, our analysis focuses on the H_2O_2 supply terms (P + C) rather than the complete mass balance equation. These terms represent the potential oxidant supply rate available for SO_2 oxidation via chemical production and horizontal transport. When comparing to regional SO_2 emissions, it is essential to use the oxidant supply rate rather than oxidant concentrations.

2.2. Machine Learning Framework and Projections. We developed an ensemble machine learning approach to identify and quantify the factors controlling sulfate formation. The ensemble incorporated four tree-based algorithms: XGBoost,[29] LightGBM,[30] Random Forest,[31] and LightGBM with DART (Dropouts meet Multiple Additive Regression Trees).[32] Tree-based methods were selected for their superior explainability properties, essential for mechanistic understanding and verification of sulfate formation driving factors. The algorithms represent complementary ensemble strategies: Random Forest reduces variance through bootstrap aggregation, XGBoost and LightGBM sequentially reduce bias through boosting, and DART incorporates dropout techniques to prevent overfitting while maintaining boosting advantages. Each algorithm's hyperparameters were systematically optimized through grid search with cross-validation. The specific parameter values are detailed in Supporting Information Table S1 and the feature names are listed in Supporting Information Table S2.

Gradient boost machine learning models can suffer from degraded performance when including too many features, particularly when some features introduce noise rather than signal.[33,34] Domain knowledge represents the most effective feature selection technique for avoiding this issue.[35,36] Our selection prioritized variables directly relevant to the H_2O_2 oxidation pathway that dominates SO_2-to-sulfate conversion in our study region.[18] Adding O_3 and OH boundary-layer columns to the machine learning models does not improve summer sulfate prediction but degrades slightly winter prediction performance. These two features also have the lowest SHAP values (Supporting Information Figure S4), demonstrating their limited explanatory power. For meteorological variables, we did not include surface wind speed, the addition of which slightly degrades the model performance.

The individual models were integrated using a stack regressor framework,[37] which optimizes the combination of base model predictions through a secondary learning process. Stack regressor frameworks excel at capturing complex, nonlinear relationships while reducing overfitting through their hierarchical learning structure and diverse base learners.[38−40] An Elastic Net model[41] was adopted as the final regressor in the stacking framework, providing an optimal balance between ridge and lasso regularization for the ensemble predictions. The complete structure of this stacked ensemble architecture is illustrated in Supporting Information Figure S5.

Model performance was evaluated through k-fold cross-validation to assess its stability and generalizability. The cross-validation results (Supporting Information Figure S6) demonstrate consistent performance across different data subsets, indicating robust model stability. The model's predictive accuracy was further validated using an independent test data set, with scatter plot analysis (Supporting Information Figure S7), revealing strong correlation between predicted and observed sulfate concentrations. Model training and validation procedures are detailed in Supporting Information Text S1. The model demonstrated consistent performance across both winter (R^2 = 0.86) and summer (R^2 = 0.88) seasons (Supporting Information Text S2). Model interpretability was analyzed through SHapley Additive exPlanations (SHAP), providing quantitative assessment of feature importance and their interactions.[42,43]

Future projections were developed using a multicomponent approach. First, power plant SO_2 emissions were obtained from Energy Information Administration Future sulfate emission projection (Supporting Information Figure S8). For the prediction of the future H_2O_2 supply rate (P+C in eq 2), we employed a linear model trained with 2004−2023 H_2O_2 primary production rate and H_2O_2 column data. These projections of both SO_2 emissions and H_2O_2 supply rate were combined with meteorological fields from the CMIP6 multimodel ensemble[44] to drive our machine learning

https://doi.org/10.1021/acs.estlett.5c00731
Environ. Sci. Technol. Lett. 2025, 12, 1190−1196

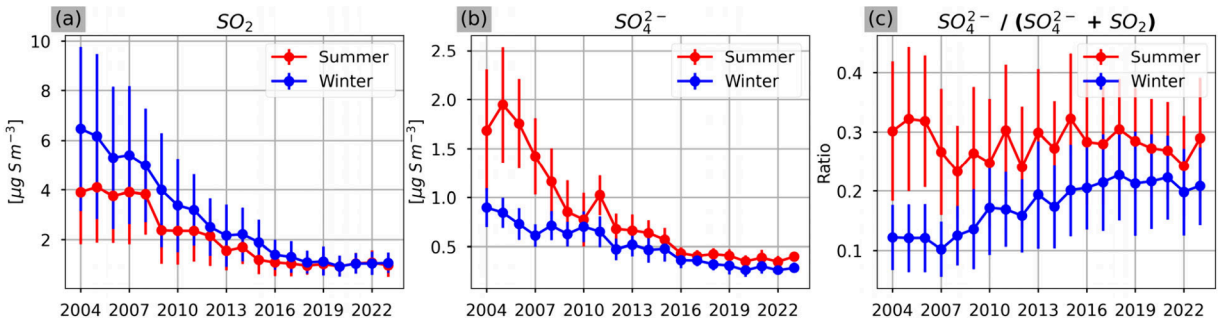

Figure 1. (a) SO_2 concentrations for winter (blue) and summer (red) from 2004 to 2023. (b) and (c) Same as (a), but for sulfate concentrations and the sulfate-to-sulfur fraction, respectively.

projections (Supporting Information Figure S9). Health impacts were evaluated using the Global Exposure Mortality Model (GEMM),[45] incorporating gridded population data (0.25° resolution) from the Gridded Population of the World v4 data set.[46]

3. RESULTS AND DISCUSSION

3.1. Long-Term Trends in SO_2 Emissions and Sulfate Concentrations. Two-decade observations of SO_2 and sulfate concentrations (2004−2023) reveal distinct patterns in the reduction of SO_2 emissions and sulfate concentrations during winter and summer. SO_2 concentrations exhibited substantial decreases in both seasons (84% in winter and 75% in summer) (Figure 1(a)). These reductions are primarily attributed to the transition from coal to natural gas in power generation[6] (Supporting Information Figure S10). Similar trends have been observed in previous studies, demonstrating substantial decreases in SO_2 levels following energy transitions in regions such as Europe[47,48] and China.[49−51] These reductions are primarily attributed to the transition from coal to natural gas in power generation.[6] The fuel transition trend was significantly influenced by natural gas prices. Temporary disruptions were observed in 2012 (due to low natural gas prices) and 2014 (due to natural gas price increases).[47,52,53]

However, the corresponding reductions in sulfate concentrations showed marked seasonal differences. Summer sulfate concentrations decreased by 80%, tracking SO_2 reductions of 75%, while winter reductions were limited to 65% considerably lower than the reduction of 84% in SO_2 concentrations (Figure 1(b)). The historic seasonal disparity in sulfate concentrations has diminished over the study period. Previous studies, such as Aas et al.,[20] have documented disparities between SO_2 and sulfate reductions, suggesting that the seasonal variation in atmospheric oxidation capacity influences sulfate formation. Our findings extend these observations by showing that the historical seasonal disparity in sulfate concentrations has diminished, driven by changing chemical regimes.

Direct comparisons are presented in Supporting Information Table S3. The reduction in wintertime SO_2 levels from 2004 to 2013 was 67% ± 16%, which is significantly higher than the reduction of 51% ± 13% from 2013 to 2023. However, the corresponding decreases in sulfate concentrations are opposite. While sulfate concentrations decreased by 40% ± 6% from 2004 to 2013, the reduction increased to 50% ± 6% from 2013 to 2023. In comparison, the summer reductions in SO_2 and sulfate levels are comparable. The lower wintertime sulfate than SO_2 reduction from 2004 to 2013 than other periods can be understood by the changing sulfate-to-total-sulfur ratios (Figure 1(c)). Summer ratios remained stable throughout the study period, indicating consistent SO_2-to-sulfate conversion efficiency. In contrast, winter ratios exhibited two distinct phases. During 2004−2013, winter conversion ratios increased by ∼50% despite SO_2 reductions, indicating a chemical buffering effect. Post-2013, the ratios stabilized to a level closer to the summer values, indicating a transition to more direct correspondence between SO_2 and sulfate reductions.

We selected 2013 as the transition year for two main reasons. First, as shown in Figure 1, the sulfate-to-total-sulfur ratio stabilized ∼0.2 beginning in 2013, indicating that SO_2 oxidation was no longer constrained by oxidant availability. Second, SO_2 emissions from power plants remained relatively steady between 2012 and 2014 (Supporting Information Figure S8). A detailed discussion of this choice and associated uncertainties is provided in Supporting Information Text S3.

3.2. Mechanistic Understanding of Seasonal Oxidation Patterns. To elucidate the mechanisms driving these seasonal patterns, we employed an ensemble machine learning approach that reproduced observed sulfate concentrations (R^2 = 0.88 and 0.86 for summer and winter averages, respectively; test data set R^2 = 0.87) (Supporting Information Figure S11). Feature importance analysis (Supporting Information Figure S12) revealed that power plant SO_2 emissions and H_2O_2 availability (both column abundance and production rate) were the primary factors controlling sulfate formation.

Supporting Information Figure S13 shows the factors influencing sulfate concentrations across two consecutive decades (2004−2013 and 2013−2023). SHAP analysis reveals that powerplant SO_2 emissions remained the predominant driver of sulfate formation throughout the study period. However, their relative importance increased substantially from 32% to 57% between the pre-2013 and post-2013 periods. The corresponding contributions of oxidant availability metrics, particularly H_2O_2 column density and H_2O_2 production rate, decreased from 18% to 13% and 18% to 9%, respectively. This temporal shift in controlling factors indicates a fundamental change in the chemical regime governing wintertime sulfate formation.

A detailed analysis of oxidant availability revealed fundamentally different chemical regimes between seasons. The winter oxidation dynamics showed a critical transition around 2013, when decreasing SO_2 emissions (from 6.5×10^8 to 3×10^7 kg/month) intersected with the relatively stable H_2O_2 availability (approximately 2.5×10^8 kg/month). This transition coincided with the stabilization of winter sulfate-to-total-sulfur ratios (Figure 1), suggesting a shift from oxidant-limited to SO_2-limited conditions for SO_2 oxidation. A similar

https://doi.org/10.1021/acs.estlett.5c00731
Environ. Sci. Technol. Lett. 2025, 12, 1190−1196

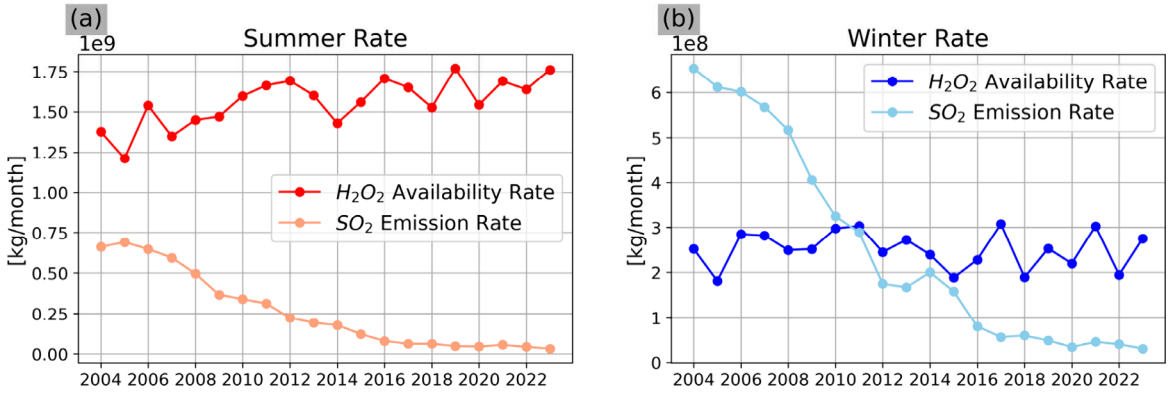

Figure 2. (a) H_2O_2 availability rate and SO_2 emission rate during summer from 2004 to 2023. (b) Same as (a), but for winter. Light-colored lines (light blue and light red) represent SO_2 emission rates, while dark-colored lines (blue and red) indicate H_2O_2 availability rate. The calculation of H_2O_2 availability is described in section 2.1.

pattern emerges when comparing column H_2O_2 to SO_2 (Supporting Information Figure S14), although the interannual variability (Supporting Information Figure S15) obscures the exact timing of the transition. 2013 marked the first year since 2004 when column H_2O_2 exceeded column SO_2 in winter. In contrast, during summer, column H_2O_2 was more than four times higher than column SO_2. The oxidant availability first exceeded SO_2 emissions in the winter of 2011, earlier than 2013. This earlier timing is likely due to uncertainties in model-simulated H_2O_2 production and transport. The sulfate-to-total-sulfur diagnostic based on observations (Figure 1) provides a more reliable indicator of the chemical regime transition (Supporting Information Text S3).

During the pre-2013 period, wintertime sulfate production was substantially constrained by limited H_2O_2 availability (oxidant-limited regime). During the post-2013 period, as SO_2 emissions declined below the oxidant supply, the system transitioned toward an SO_2-limited regime, evidenced by the diminished importance of H_2O_2-related variables. This finding explains the damping effect of wintertime sulfate reductions: a low efficacy of SO_2 emission reduction on reducing sulfate concentrations, i.e., the reduction of sulfate lagged behind that of SO_2 emissions, when SO_2 oxidation transitioned from the oxidant-limited into SO_2-limited regime. In contrast, the summertime H_2O_2 production rates consistently exceeded SO_2 emission rates, with boundary layer H_2O_2 column abundances more than four times higher than SO_2 columns (Figure 2). This oxidant-rich environment enables efficient SO_2-to-sulfate conversion, explaining the near-linear response of summer sulfate concentrations to SO_2 reductions.

The analysis result presented here is consistent with the model simulations by Shah et al.[54] showing the SO_2 oxidation was H_2O_2-limited in 2007. Shah et al. also simulated this chemical damping effect that reduced the efficacy of SO_2 emission reduction from 2007 to 2015. However, their simulations appeared to suggest that this chemical damping effect would extend from 2015 to 2023, which was not supported by the observations. The detailed comparison between this study and the previous work by Shah et al.[54] is described in Supporting Information Text S4.

3.3. Future Projections and Policy Implications. Machine learning projections indicate continuing convergence of winter and summer sulfate levels, suggesting that SO_2 emission controls will achieve comparable efficacy across seasons in the future (Supporting Information Figure S16). This aligns with findings from other CMIP6-based studies, such as Turnock et al.,[55] which project global declines in sulfate concentrations under scenarios with strong air quality and climate mitigation measures. However, the rate of improvement is expected to slow, reflecting the already substantial reductions achieved in SO_2 emissions. This projected convergence reflects a consistent SO_2 oxidation regime in winter and summer in the future. Our projections are broadly consistent with previous studies using chemical transport models,[56,57] which estimate a 3- to 4-fold decrease in sulfate concentrations between 2000 and 2030 or 2050. Similarly, our results align with sulfate trends projected under the SSP2−4.5 scenario in CMIP6.[58]

Health impact assessments using the GEMM model project declining mortality rates from sulfate exposure, with seasonal differences in health impacts expected to diminish by 2045 (Supporting Information Figure S17). Our analysis provides an explanation for the nonlinear relationship between SO_2 emission reductions and resulting sulfate concentrations through the chemical regime transition framework. This nonlinearity in the SO_2-to-sulfate conversion process ultimately affects health outcomes, as previously noted by Burnett et al.[45] and Zhao et al.,[59] who observed that emission reductions do not translate to proportional improvements in health impacts. The gradual elimination of seasonal disparities in health impacts aligns with our mechanistic understanding of the chemical regime transition and suggests that future air quality management strategies may no longer need to consider seasonal variations in control efficacy. These findings have important implications for regions heavily reliant on coal power generation, suggesting that initial emission control efforts may face reduced efficacy due to similar chemical buffering effects until oxidant-limited conditions are overcome.

The observations of SO_2 and sulfate across the Rust Belt and Southeast of the United States from 2004 to 2023 show two distinct stages in the response of sulfate to SO_2 reductions in winter. In the initial stage prior to 2013, the reduction of sulfate lagged significantly behind that of SO_2 due to an increasing conversion ratio of SO_2 to sulfate. During this period, the oxidation of SO_2 to sulfate is limited by the oxidant supply. Consequently, the fraction of sulfate out of total sulfur increased as SO_2 emission decreased. By 2013, the oxidant supply reached the level of SO_2 emissions and further SO_2 reduction meant an oversupply of oxidants and therefore the sulfur fraction stabilized after a ∼50% increase from the 2004

https://doi.org/10.1021/acs.estlett.5c00731
Environ. Sci. Technol. Lett. 2025, 12, 1190−1196

level. Post 2013, the reduction of sulfate in winter is proportional to that of SO_2, comparable to the summer seasons from 2004 to 2023 when there is always an oversupply of oxidants.

The substantially lower wintertime sulfate reduction relative to that of SO_2 from 2004 to 2013 than from 2013 to 2024 or the 2004−2023 summer seasons reflects a chemical damping effect due to the limited supply of oxidants. This mechanism may delay the reduction in sulfate concentrations in other polluted regions where the transition from coal to natural gas in power plants or alternative energy sources has not progressed as rapidly as in the United States. These findings contribute to a more nuanced understanding of atmospheric chemistry dynamics and may inform more effective emission control policies, particularly in regions currently experiencing high SO_2 emissions where similar chemical damping effects may initially limit control efficacy.

■ ASSOCIATED CONTENT

Supporting Information

The Supporting Information is available free of charge at https://pubs.acs.org/doi/10.1021/acs.estlett.5c00731.

Time series data of SO_2 and sulfate concentrations from monitoring stations (2004−2023); machine learning model architecture and validation procedures; seasonal oxidation efficiency analyses; correlation matrices for oxidant availability and sulfate formation rates; regional emission reduction impact assessments; model performance metrics and sensitivity analyses (PDF)

■ AUTHOR INFORMATION

Corresponding Author

Yuhang Wang − *Georgia Institute of Technology, School of Earth and Atmospheric Sciences, Atlanta, Georgia 30332, United States;* orcid.org/0000-0002-7290-2551; Email: yuhang.wang@eas.gatech.edu

Authors

Fanghe Zhao − *Georgia Institute of Technology, School of Earth and Atmospheric Sciences, Atlanta, Georgia 30332, United States;* orcid.org/0009-0000-1317-1368

Shengjun Xi − *Georgia Institute of Technology, School of Earth and Atmospheric Sciences, Atlanta, Georgia 30332, United States;* orcid.org/0009-0002-6939-6894

Complete contact information is available at: https://pubs.acs.org/10.1021/acs.estlett.5c00731

Notes

The authors declare no competing financial interest.

■ ACKNOWLEDGMENTS

We would like to acknowledge high-performance computing support from the Derecho system (http://doi.org/10.5065/qx9a-pg09) provided by the NSF National Center for Atmospheric Research (NCAR), sponsored by the National Science Foundation.

■ REFERENCES

(1) Taylor, M. R.; Rubin, E. S.; Hounshell, D. A. Control of SO2 emissions from power plants: A case of induced technological innovation in the U.S. *Technological Forecasting and Social Change* **2005**, *72* (6), 697−718.

(2) Lippmann, M.; Thurston, G. D. Sulfate concentrations as an indicator of ambient particulate matter air pollution for health risk evaluations. *J. Expo Anal Env Epid* **1996**, *6* (2), 123−146.

(3) Zhang, Q.; Wang, Y.; Liu, M.; Zheng, M.; Yuan, L.; Liu, J.; Tao, S.; Wang, X. Wintertime Formation of Large Sulfate Particles in China and Implications for Human Health. *Environ. Sci. Technol.* **2023**, *57* (48), 20010−20023.

(4) Wang, Y.; Xi, S.; Zhao, F.; Huey, L. G.; Zhu, T. Decreasing Production and Potential Urban Explosion of Nighttime Nitrate Radicals amid Emission Reduction Efforts. *Environ. Sci. Technol.* **2023**, *57* (50), 21306−21312.

(5) Grahame, T. J.; Schlesinger, R. B. Evaluating the health risk from secondary sulfates in eastern North American regional ambient air particulate matter. *Inhal Toxicol* **2005**, *17* (1), 15−27.

(6) de Gouw, J. A.; Parrish, D. D.; Frost, G. J.; Trainer, M. Reduced emissions of CO, NOx, and SO from U.S. power plants owing to switch from coal to natural gas with combined cycle technology. *Earth's. Future* **2014**, *2* (2), 75−82.

(7) Karplus, V. J.; Zhang, S.; Almond, D. Quantifying coal power plant responses to tighter SO $_2$ emissions standards in China. *Proc. Natl. Acad. Sci. U. S. A.* **2018**, *115* (27), 7004−7009.

(8) Zhang, R.; Wang, G.; Guo, S.; Zamora, M. L.; Ying, Q.; Lin, Y.; Wang, W.; Hu, M.; Wang, Y. Formation of Urban Fine Particulate Matter. *Chem. Rev.* **2015**, *115* (10), 3803−3855.

(9) Bhattarai, H.; Tai, A. P. K.; Val Martin, M.; Yung, D. H. Y. Responses of fine particulate matter (PM2.5) air quality to future climate, land use, and emission changes: Insights from modeling across shared socioeconomic pathways. *Science of The Total Environment* **2024**, *948*, No. 174611.

(10) Hand, J. L.; Schichtel, B. A.; Malm, W. C.; Pitchford, M. L. Particulate sulfate ion concentration and SO $_2$ emission trends in the United States from the early 1990s through 2010. *Atmospheric Chemistry and Physics* **2012**, *12* (21), 10353−10365.

(11) Paulot, F.; Fan, S.; Horowitz, L. W. Contrasting seasonal responses of sulfate aerosols to declining SO2 emissions in the Eastern U.S.: Implications for the efficacy of SO2 emission controls. *Geophys. Res. Lett.* **2017**, *44* (1), 455−464.

(12) Henneman, L.; Choirat, C.; Dedoussi, I.; Dominici, F.; Roberts, J.; Zigler, C. Mortality risk from United States coal electricity generation. *Science* **2023**, *382* (6673), 941−946.

(13) Liu, T.; Chan, A. W. H.; Abbatt, J. P. D. Multiphase Oxidation of Sulfur Dioxide in Aerosol Particles: Implications for Sulfate Formation in Polluted Environments. *Environ. Sci. Technol.* **2021**, *55* (8), 4227−4242.

(14) Eatough, D. J.; Caka, F. M.; Farber, R. J. The Conversion of SO2 to Sulfate in the Atmosphere. *Isr. J. Chem.* **1994**, *34* (314), 301.

(15) Liu, X.; Penner, J. E.; Herzog, M. Global modeling of aerosol dynamics: Model description, evaluation, and interactions between sulfate and nonsulfate aerosols. *Journal of Geophysical Research: Atmospheres* **2005**, *110* (D18), 1.

(16) Khoder, M. I. Atmospheric conversion of sulfur dioxide to particulate sulfate and nitrogen dioxide to particulate nitrate and gaseous nitric acid in an urban area. *Chemosphere* **2002**, *49* (6), 675−684.

(17) Liu, P.; Jia, S.; Li, S.; Ma, P.; Ma, Y.; Liu, Y.; Liao, Z.; Wang, Y.; Chu, B.; Ma, Q.; et al. Unexpectedly High Levels of H2O2 Drive Sulfate Formation over the Residual Layer in Beijing. *Environ. Sci. Technol.* **2025**, *59* (9), 4551−4559.

(18) Gao, J.; Wang, H.; Liu, W.; Xu, H.; Wei, Y.; Tian, X.; Feng, Y.; Song, S.; Shi, G. Hydrogen peroxide serves as pivotal fountainhead for aerosol aqueous sulfate formation from a global perspective. *Nature Communications* **2024**, *15* (1), 4625.

(19) *Benefits and Costs of the Clean Air Act from 1990 to 2020: Summary Report*; U.S. Environmental Protection Agency Office of Air and Radiation, 2011. https://www.epa.gov/sites/default/files/2015-07/documents/summaryreport.pdf.

(20) Aas, W.; Mortier, A.; Bowersox, V.; Cherian, R.; Faluvegi, G.; Fagerli, H.; Hand, J.; Klimont, Z.; Galy-Lacaux, C.; Lehmann, C. M.

B. Global and regional trends of atmospheric sulfur. *Sci. Rep.* **2019**, *9* (1), 1.
(21) Mueller, S. F. Seasonal Aerosol Sulfate Trends for Selected Regions of the United States. *Journal of the Air & Waste Management Association* **2003**, *53* (2), 168−184.
(22) Malm, W. C.; Sisler, J. F.; Huffman, D.; Eldred, R. A.; Cahill, T. A. Spatial and seasonal trends in particle concentration and optical extinction in the United States. *Journal of Geophysical Research: Atmospheres* **1994**, *99* (D1), 1347−1370.
(23) Colorado State University. *Federal Land Manager Environmental Database (FED)*. 2020. https://views.cira.colostate.edu/fed (accessed 2025 2025/03/04).
(24) Hand, J. *IMPROVE (Interagency Monitoring of Protected Visual Environments): Spatial and seasonal patterns and temporal variability of haze and its constituents in the United States Report VI*; Colorado State University: 2023.
(25) Hand, J. L.; Prenni, A. J.; Schichtel, B. A.; Malm, W. C.; Chow, J. C. Trends in remote PM2.5 residual mass across the United States: Implications for aerosol mass reconstruction in the IMPROVE network. *Atmos. Environ.* **2019**, *203*, 141−152.
(26) Inness, A.; Ades, M.; Agustí-Panareda, A.; Barré, J.; Benedictow, A.; Blechschmidt, A.-M.; Dominguez, J. J.; Engelen, R.; Eskes, H.; Flemming, J.; et al. The CAMS reanalysis of atmospheric composition. *Atmospheric Chemistry and Physics* **2019**, *19* (6), 3515−3556.
(27) Hersbach, H.; Bell, B.; Berrisford, P.; Hirahara, S.; Horányi, A.; Muñoz-Sabater, J.; Nicolas, J.; Peubey, C.; Radu, R.; Schepers, D.; et al. The ERA5 global reanalysis. *Quarterly Journal of the Royal Meteorological Society* **2020**, *146* (730), 1999−2049.
(28) Burkholder, J. B.; Abbatt, J.; Barker, J. R.; Cappa, C.; Crounse, J. D.; Dibble, T. S.; Huie, R. E.; Kolb, C. E.; Kurylo, M. J.; Percival, C. J.; Wilmouth, D. M.; Wine, P. H.. *Chemical Kinetics and Photochemical Data for Use in Atmospheric Studies, Evaluation No. 19*; Jet Propulsion Laboratory: 2019. http://jpldataeval.jpl.nasa.gov.
(29) Chen, T.; Guestrin, C. XGBoost: A Scalable Tree Boosting System. *ACM* **2016**, *11*, 785−794. 2016;
(30) Ke, G.; Meng, Q.; Finley, T.; Wang, T.; Chen, W.; Ma, W.; Ye, Q.; Liu, T.-Y. LightGBM: A Highly Efficient Gradient Boosting Decision Tree. *Advances in Neural Information Processing Systems*; Guyon, I.; Von Luxburg, U.; Bengio, S.; Wallach, H.; Fergus, R.; Vishwanathan, S.; Garnett, R., Eds.; Curran Associates, Inc., 2017; Vol. *30*.
(31) Breiman, L. Random Forests. *Machine Learning* **2001**, *45* (1), 5−32.
(32) Vinayak, R. K.; Gilad-Bachrach, R. Dart: Dropouts meet multiple additive regression trees. In *Artificial Intelligence and Statistics*; PMLR: 2015; pp 489−497.
(33) Blagus, R.; Lusa, L. Gradient boosting for high-dimensional prediction of rare events. *Computational Statistics & Data Analysis* **2017**, *113*, 19−37.
(34) Li, J.; Liu, H. Challenges of feature selection for big data analytics. *IEEE Intelligent Systems* **2017**, *32* (2), 9−15.
(35) Yousef, M.; Kumar, A.; Bakir-Gungor, B. Application of Biological Domain Knowledge Based Feature Selection on Gene Expression Data. *Entropy* **2021**, *23* (1), 2.
(36) Liu, Y.; Zou, X.; Ma, S.; Avdeev, M.; Shi, S. Feature selection method reducing correlations among features by embedding domain knowledge. *Acta Mater.* **2022**, *238*, No. 118195.
(37) Breiman, L. Stacked regressions. *Machine Learning* **1996**, *24* (1), 49−64.
(38) Pławiak, P.; Abdar, M.; Pławiak, J.; Makarenkov, V.; Acharya, U. R. DGHNL: A new deep genetic hierarchical network of learners for prediction of credit scoring. *Information sciences* **2020**, *516*, 401−418.
(39) Gupta, H.; Vincent, R.; Rajakumaran, G.; Sultana, A. Stacked Regressor for Crop Yield Prediction. *2024 International Conference on Computing and Data Science (ICCDS)* **2024**, 1−6.
(40) Zhang, T.; Gupta, A.; Rodríguez, M. A. F.; Spjuth, O.; Hellander, A.; Toor, S. Data management of scientific applications in a reinforcement learning-based hierarchical storage system. *Expert Systems with Applications* **2024**, *237*, No. 121443.
(41) Zou, H.; Hastie, T. Regularization and Variable Selection Via the Elastic Net. *Journal of the Royal Statistical Society Series B: Statistical Methodology* **2005**, *67* (2), 301−320.
(42) Lundberg, S.; Lee, S.-I. A Unified Approach to Interpreting Model Predictions. *arXiv*; 2017; pp 4765−4774. .
(43) Lundberg, S. M.; Erion, G.; Chen, H.; DeGrave, A.; Prutkin, J. M.; Nair, B.; Katz, R.; Himmelfarb, J.; Bansal, N.; Lee, S.-I. From local explanations to global understanding with explainable AI for trees. *Nature Machine Intelligence* **2020**, *2* (1), 56−67.
(44) Stockhause, M.; Matthews, R.; Pirani, A.; Treguier, A. M.; Yelekci, O. CMIP6 data documentation and citation in IPCC's Sixth Assessment Report (AR6). *In EGU General Assembly Conference Abstracts* **2021**, EGU21−2886.
(45) Burnett, R.; Chen, H.; Szyszkowicz, M.; Fann, N.; Hubbell, B.; Pope, C. A.; Apte, J. S.; Brauer, M.; Cohen, A.; Weichenthal, S.; et al. Global estimates of mortality associated with long-term exposure to outdoor fine particulate matter. *Proc. Natl. Acad. Sci. U. S. A.* **2018**, *115* (38), 9592−9597.
(46) Center for International Earth Science Information Network - CIESIN. *Gridded Population of the World, Version 4.11 (GPWv4): Population Count*; Columbia University: 2018. https://sedac.ciesin.columbia.edu/downloads/metadata/gpw-v4-population-count-rev11.html (accessed 2025/03/04).
(47) Zhukov, S.; Reznikova, O. Energy transition in the United States, Europe and China: latest trends. *Studies on Russian Economic Development* **2023**, *34* (4), 439−449.
(48) Wieczorek, B. Air pollution patterns mapping of SO2, NO2, and CO derived from TROPOMI over Central-East Europe. *Remote Sensing* **2023**, *15* (6), 1565.
(49) Wang, S.; Su, H.; Chen, C.; Tao, W.; Streets, D. G.; Lu, Z.; Zheng, B.; Carmichael, G. R.; Lelieveld, J.; Pöschl, U.; et al. Natural gas shortages during the "coal-to-gas" transition in China have caused a large redistribution of air pollution in winter 2017. *Proc. Natl. Acad. Sci. U. S. A.* **2020**, *117* (49), 31018−31025.
(50) Xu, C.; Zhao, W.; Zhang, M.; Cheng, B. Pollution haven or halo? The role of the energy transition in the impact of FDI on SO2 emissions. *Sci. Total Environ.* **2021**, *763*, No. 143002.
(51) Zhao, S.; Lu, J.; Yan, J.; Wu, H.; Guan, C. Energy transition in China: It is necessary to increase natural gas utilization. *Energy Reports* **2023**, *10*, 2439−2447.
(52) Alhajeri, N. S.; Dannoun, M.; Alrashed, A.; Aly, A. Z. Environmental and economic impacts of increased utilization of natural gas in the electric power generation sector: Evaluating the benefits and trade-offs of fuel switching. *Journal of Natural Gas Science and Engineering* **2019**, *71*, No. 102969.
(53) Knittel, C. R.; Metaxoglou, K.; Trindade, A. Natural Gas Prices and Coal Displacement: Evidence from Electricity Markets. *National Bureau of Economic Research Working Paper Series* **2015**, 21627.
(54) Shah, V.; Jaeglé, L.; Thornton, J. A.; Lopez-Hilfiker, F. D.; Lee, B. H.; Schroder, J. C.; Campuzano-Jost, P.; Jimenez, J. L.; Guo, H.; Sullivan, A. P.; et al. Chemical feedbacks weaken the wintertime response of particulate sulfate and nitrate to emissions reductions over the eastern United States. *Proc. Natl. Acad. Sci. U. S. A.* **2018**, *115* (32), 8110−8115.
(55) Turnock, S. T.; Allen, R. J.; Andrews, M.; Bauer, S. E.; Deushi, M.; Emmons, L.; Good, P.; Horowitz, L.; John, J. G.; Michou, M.; et al. Historical and future changes in air pollutants from CMIP6 models. *Atmos. Chem. Phys.* **2020**, *20* (23), 14547−14579.
(56) Pye, H. O. T.; Liao, H.; Wu, S.; Mickley, L. J.; Jacob, D. J.; Henze, D. K.; Seinfeld, J. H. Effect of changes in climate and emissions on future sulfate-nitrate-ammonium aerosol levels in the United States. *Journal of Geophysical Research: Atmospheres* **2009**, *114* (D1), 1.
(57) Saikawa, E.; Naik, V.; Horowitz, L. W.; Liu, J.; Mauzerall, D. L. Present and potential future contributions of sulfate, black and organic carbon aerosols from China to global air quality, premature

mortality and radiative forcing. *Atmos. Environ.* **2009**, *43* (17), 2814−2822.
(58) Bergas-Massó, E.; Gonçalves Ageitos, M.; Myriokefalitakis, S.; Miller, R. L.; van Noije, T.; Le Sager, P.; Montané Pinto, G.; Pérez García-Pando, C. Pre-Industrial, Present and Future Atmospheric Soluble Iron Deposition and the Role of Aerosol Acidity and Oxalate Under CMIP6 Emissions. *Earth's Future* **2023**, *11* (6), e2022EF003353.
(59) Zhao, B.; Wang, S.; Ding, D.; Wu, W.; Chang, X.; Wang, J.; Xing, J.; Jang, C.; Fu, J. S.; Zhu, Y.; et al. Nonlinear relationships between air pollutant emissions and PM2.5-related health impacts in the Beijing-Tianjin-Hebei region. *Science of The Total Environment* **2019**, *661*, 375−385.

https://doi.org/10.1021/acs.estlett.5c00731
Environ. Sci. Technol. Lett. 2025, 12, 1190−1196